JCTC Journal of Chemical Theory and Computation

Trends in Energies and Geometric Structures of Neutral and Charged Aluminum Clusters†

René Fournier*

Department of Chemistry, York University, 4700 Keele Street, Toronto, Ontario M3J 1P3, Canada

Received December 21, 2006

Abstract: The minimum energy geometric structures of Al_n, Al_n^-, and Al_n^+ ($4 \le n \le 15$) are predicted from the results of "Tabu Search" (TS) global optimizations performed directly on the BPW91/LANL2DZ potential energy surface. In 24 of the 36 cases investigated, the TS delivered a lower energy structure than previously reported, in one case (Al_{12}^+) it failed to find the global minimum, and in the remaining 11 cases TS confirmed previous structures. All clusters (with $4 \le n \le 15$) have the lowest spin state as their ground state except Al_4 (triplet), Al_4^+ (quartet), Al_7^- (triplet), and maybe Al_5^+ (singlet and triplet are degenerate). The 20-electron Al_7^+ and 40-electron Al_{13}^- clusters are relatively stable compared to other clusters, on several criteria; to a lesser degree, Al_7, Al_{12}, and Al_{13}^+ are also stable.

I. Introduction

Structure determination of clusters is a tough, and still mostly unsolved, problem for both theory and experiment. There are two main sources of difficulty for theory. First, there is a huge number of local minima. With Lennard-Jones (LJ) potential interatomic interactions, the number of local minima of n-atom clusters[1] for $n > 6$ is roughly on the order of $2.7^{(n-5.7)}$. Second, there is a lack of guiding principles in most cases, C_n fullerenes being a notable exception. In order to make meaningful comparisons of calculated properties to experiments, which are often done on clusters in a size range from $n = 2$ up to $n = 30$ and sometimes more, one must attempt global optimization on energy surfaces with very many local minima. A common approach is to first find the lowest energy structures on a model energy surface which could be, for instance, an empirical potential function or a tight-binding energy method. With a simple model, tens of thousands of energy evaluations are possible, and a good global optimization technique like genetic algorithm[2] is likely to find the global minimum (GM) *of the model energy surface* and, in the process, will generate many candidates for the GM of higher level theory energy surfaces. Problems arise when the energy model is unreliable and has low-energy structures that are qualitatively different from those of a better theory. This is, of course, very difficult to know beforehand. Another strategy, which we take here, is to perform the global search directly on the energy surface of a first-principles method, in this case Kohn−Sham Density Functional Theory (KS-DFT) with a generalized gradient approximation (GGA) to exchange-correlation. The problem with this approach is that the high cost of KS-DFT will typically prevent calculating more than a few thousand energies, and this is probably less than the number of local minima at $n \ge 12$.

We have developed a meta-algorithm, called Tabu Search in Descriptor Space (TSDS), to do global optimization efficiently for certain types of clusters. Descriptions can be found for Tabu Search algorithms in general[3] and specifically for TSDS optimization of clusters.[4] Briefly, the key ideas of TSDS are as follows: (i) the only structures that are ever considered are *near* local minima, (ii) each of those structures has its energy evaluated only once or a few times at most, and (iii) a small number (typically 4−7) of structural descriptors such as mean coordination and moments of inertia are used by the algorithm to gradually "learn", as the search progresses, about regions of descriptor space where local minima are deeper and the chance of finding the GM higher. The user supplied descriptors constitute a crude form of expert knowledge, and, if they are well chosen, they help the algorithm avoid large portions of the energy surface in the later stages of the search. For instance TSDS would consider any structure at the beginning of a search, but, for

† Dedicated to Professor Dennis R. Salahub on the occasion of his 60th birthday.

* Corresponding author e-mail: renef@yorku.ca.

10.1021/ct6003752 CCC: $37.00
Published on Web 04/05/2007

most metal clusters, it would avoid structures that have a very low mean atomic coordination (or, equivalently, a very high surface area) toward the end of the search. Yet the search is only weakly biased by the choice of descriptors because the correlation between low energy and specific values of descriptors is not assumed or predefined, it is gradually learned during the search.

We tested the performance of TSDS on model systems such as LJ clusters.[4] We also made limited use of an early version of TSDS for minimization of Li_n and Be_n cluster structures on first-principles energy surfaces.[5,6] Reported here are results of systematically applying TSDS to a series of Al_n neutral and charged clusters. We chose the Al_n series because it has been extensively studied and because KS-DFT calculations are relatively fast for Al_n. Experimental results were published for ionization energies (IE),[7] electron affinities (EA),[8] and fragmentation channels.[9] There is also indirect evidence about Al cluster structure coming from experimental studies of relative abundances and reactivity of charged Al clusters.[10,11] A thorough theoretical study of Al_n, Al_n^+, Al_n^- ($2 \leq n \leq 15$) was done by Rao and Jena.[12] They used the BPW91/LANL2DZ method (described in the next section) and searched for the GM by doing several local optimizations starting with initial structures that were obtained by global optimization on a simpler model energy surface, or from published results on other clusters, or by an educated guess. They did a detailed comparison of their calculated electronic properties to experiment and generally found good agreement. We chose to use the same energy method because it looks adequate for Al clusters and because repeating the search for GM on the same energy surface but with TSDS would show to what degree the global optimization method matters for structure determination and prediction of cluster properties. There have been many other theoretical studies of aluminum clusters as well.[13−19] This makes aluminum one of the best characterized series of metal clusters to date and a good testing ground for computational methods.

II. Computational Details

Energy minimizations were all done by Tabu Search in Descriptor Space (TSDS) global optimization with a local spin density functional (SVWN5 Gaussian keyword), followed by many local optimizations with the BPW91 functional, and then by characterizing the lowest energy minimum by calculation of energy second derivatives and vibrational frequencies. All energies were evaluated by KS-DFT with the exchange-correlation functional of Becke, Perdew, and Wang (referred to as "BPW91") and a LANL2DZ basis set, and the Gaussian03 software was used.[20] This is the same method for energy evaluation as used in a previous study,[12] and indeed the energies we get for atoms and other small species where geometries are identical agree to within 10^{-5} au.

No method can ever guarantee to find the GM, but so far our experience[4−6] indicates that TSDS can find good approximate solutions to GM problems at a relatively small computational cost. In this study, the number of energy evaluations done in the TSDS part were only 120 for $n = 5$, 550 for $n = 10$, and 800 for $n = 15$, and the number of local optimizations, each of which requires many energy evaluations, varied between 10 and 20. The total number of energy evaluations was on the order of 3000 or less for the largest clusters ($n = 13-15$), and roughly half of the computational effort went into doing local optimizations.

III. Results and Discussion

A. Geometric Structures. The GM are displayed in Figure 1, and their energies are listed in Table 1. The neutral and anionic clusters often have the same, or similar, structures. Cationic clusters are very different, and they often adopt much more open structures. One of the most surprising results is that we found many structures with energy lower than previously reported[12] even for very small clusters. They are, with energy lowering, shown in parentheses: Al_4^+ (−0.02 eV), Al_5^- (−0.01 eV), Al_6 (−0.33 eV), Al_6^+ (−0.28 eV), Al_6^- (−0.13 eV), Al_7^- (−0.04 eV), Al_8 (−0.32 eV), Al_8^+ (−0.10 eV). For Al_5^+ we found not only the same triplet GM as Rao and Jena but also a singlet which is the structure we show in Figure 1. This singlet is essentially degenerate with the triplet, the energy difference is less than 0.001 eV. One might have thought that global optimization can be done by trial-and-error for $n \leq 8$, because there are only 8 minima on the LJ energy surface at $n = 8$. Theoretical studies, including our own, have often payed scant attention to the global minimum problem when clusters with 8 or fewer atoms are concerned. But atoms of most elements have interactions that are much more complicated than a Lennard-Jones potential. The number of local minima is most likely larger in Al_n than LJ_n clusters, especially considering that more than one energy surface (spin state) must sometimes be searched. Note that there is a lot of variety among structures in Figure 1, and many of them are distorted, or have low symmetry, or display big variations among coordinations of the different atoms. Those types of structures are normally not minima, or at least not low-lying minima, on the energy surfaces of pairwise additive potentials or embedded atom method (EAM) and similar models. Of the 36 GM shown in Figure 1, 24 constitute an improved (lower energy) structure relative to previous work.[12] The energy lowering is at least 0.01 eV in every case, it is smaller than 0.10 eV in 9 of the 24 cases, and it is larger than 0.30 eV in 6 cases. The energy lowering is 0.19 eV on average. In one case, Al_{12}^+, TSDS missed the GM and found instead a structure that is 0.10 eV higher than that of Rao and Jena[12] (an icosahedron with a missing peripheral atom).

Generally, the structures that we found (Figure 1) differ in two ways from those reported previously.[12] First, there are more differences among the neutral, cation, and anion of a given n in our set of results. It is understandable because differences in the electronic structures of the neutral and charged clusters are implicitly taken into account at every stage of each TSDS optimization, whereas it comes into play only in the second step of a two-step approach to global optimization. Second, there are many more instances of atoms having a coordination of less than 4 in our structures, even at large n, and those atoms are often part of a quasi-

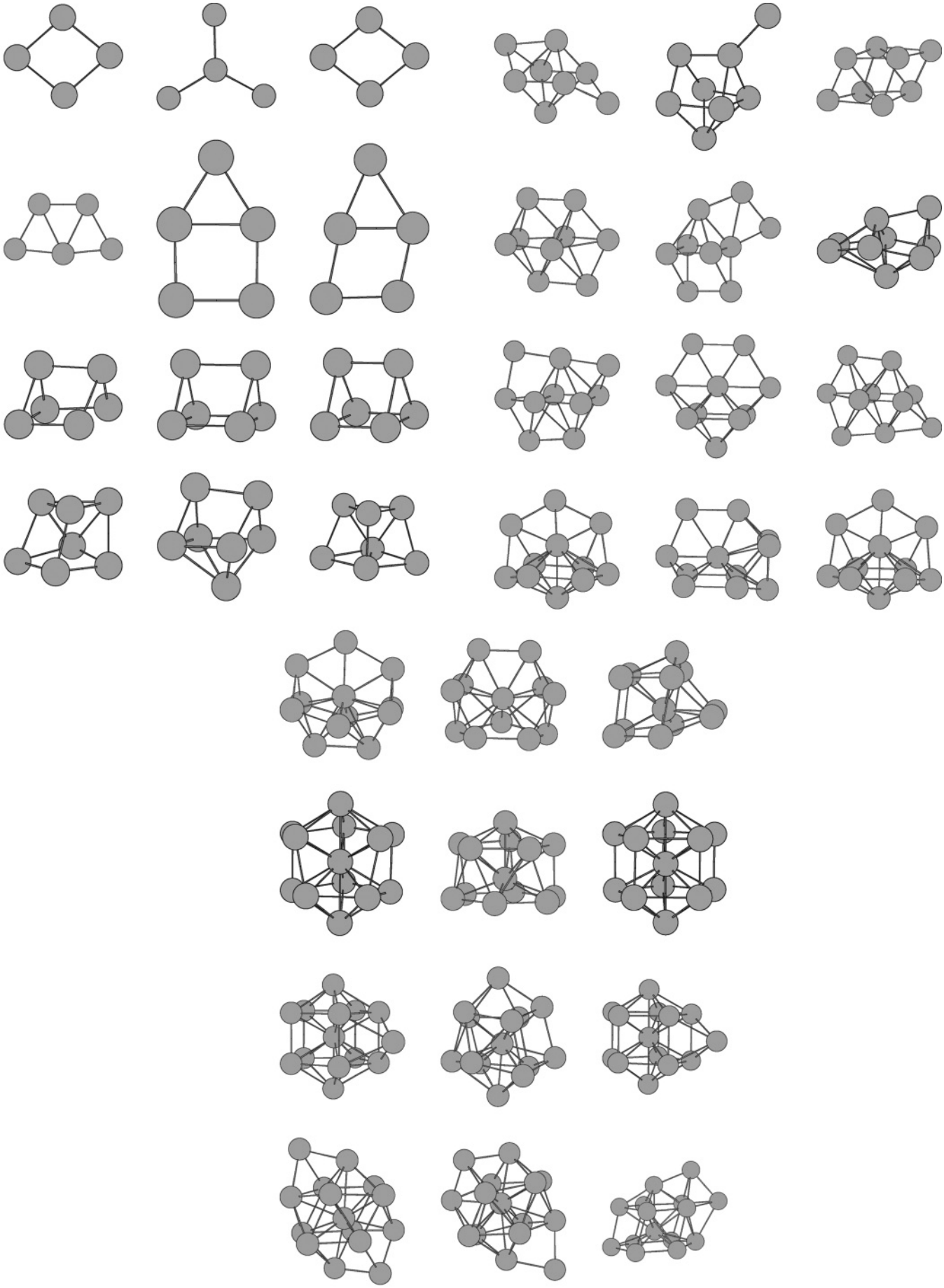

Figure 1. Ground-state geometries found by TSDS optimization on the BPW91/LANL2DZ energy surface for neutral, cationic, and anionic aluminum clusters.

Table 1. Total BPW91/LANL2DZ Energies (au) of Al_n, Al_n^+, and Al_n^- in their Lowest Energy Structure and Spin State and Vertical Ionization Energy (VIE) of the Neutral in eV

n	*E*(0)	*E*(+)	*E*(−)	VIE
4	−7.956638	−7.718496	−8.034917	6.70
5	−9.980356	−9.737493	−10.056436	6.73
6	−12.002416	−11.763381	−12.089263	6.62
7	−14.047646	−13.831830	−14.123844	6.19
8	−6.065227	−5.832956	−16.147627	6.55
9	−18.080750	−17.856885	−18.180257	6.51
10	−20.114445	−19.891054	−20.206009	6.39
11	−22.141527	−21.930017	−22.244191	6.29
12	−24.190858	−23.963704	−24.277649	6.36
13	−26.227981	−6.017113	−26.340839	6.35
14	−28.258926	−28.050969	−28.343463	6.17
15	−30.275220	−30.072363	−30.371095	5.87

planar 4-atom diamond, or 5-atom rhombus, unit. This is seen in Al_{15}^+, Al_{12}, Al_{11}, Al_{11}^+, Al_{11}^-, and Al_8^+.

We will now compare the structures of Figure 1 to the GM found in other theoretical studies. The GM predicted by a Voter-Chen version of the embedded atom model (EAM) potential in the size range 4−15[14] are *all different* from our GM structures. Another study based on a different empirical potential (Murrell-Mottram 2 + 3-body potential)[15] predicts GM structures similar to those of the Voter-Chen EAM potential for $n = 4-7$ and $n = 11-14$. Again, *none* of those structures agree with the BPW91 GM (Figure 1). Both potentials predict structures that are more compact and have higher symmetry than those of Figure 1. The only resemblance are for Al_{13} and Al_{14}: the empirical potentials predict them to be an icosahedron and a capped icosahedron, and BPW91 predicts them to be a decahedron and a capped decahedron. Empirical potentials for metals are often fitted to bulk properties and tend to favor cluster structures that have high, or even maximal, coordination. But KS-DFT calculations show that there are important changes in local electronic structure as atomic coordination changes,[13] and it is hard to model these things, and the associated changes in bond energies, with an empirical function. The characteristic density of states of metallic aluminum is almost fully developed only when the number of atoms in Al clusters reaches 25.[13] It is doubtful that empirical potentials can give accurate energies and structures in clusters smaller than that.

Our structures agree much better with other first-principles studies. Jones used DFT with a local spin density (LSD) exchange-correlation functional and plane wave basis and did simulated annealing to search the GM of Al_n, $n = 3-10$.[16] The structures he found for $n = 4-6$, 9 are similar to ours. However, what we find as the GM of Al_6 (trigonal prism, singlet) is a higher energy isomer on the LSD potential surface, it is 0.35 eV above the GM (a D_{3d} trigonal antiprism).[16] Jones found many low-lying minima having comparable energies at $n = 8-10$, in qualitative agreement with us (Figure 4). Given the large number of isomers, and different functionals, it is remarkable that we find the same GM for Al_9 as Jones.[16] Akola et al. also used LSD with a plane wave basis and searched the potential surface of Al_n ($n = 3-7$) by molecular dynamics followed by local optimization (conjugate gradient method) on many plausible candidates.[18] For larger clusters, ($n = 12-23$) they used a potential derived from effective medium theory to generate plausible candidates and then carried local optimizations on those by LSD. It is hard to make a comparison because most of their GM structures are not shown, but their predicted GM are apparently quite different from ours. First, the symmetry group of their small clusters match our structures for $n = 4$, 5 but not $n = 6$, 7. Second, they describe the GM of $n = 12-23$ clusters as being "icosahedral-based structures", but only one of our GM (Al_{15}) is based on the icosahedron. Sun et al. used the B3LYP hybrid functional to study Al_n and Al_nO, $n = 2-10$.[17] They do not describe their GM search method except to say that different initial

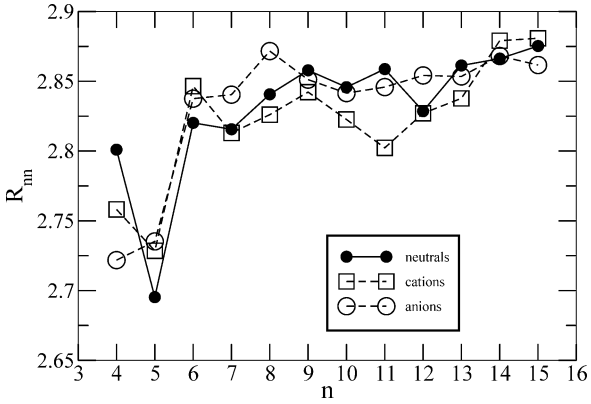

Figure 2. Average of nearest-neighbor distances (Å) in neutral and charged aluminum clusters.

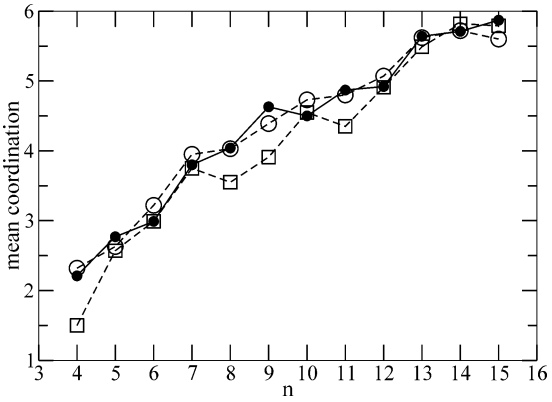

Figure 3. Mean atomic coordination in neutral and charged aluminum clusters.

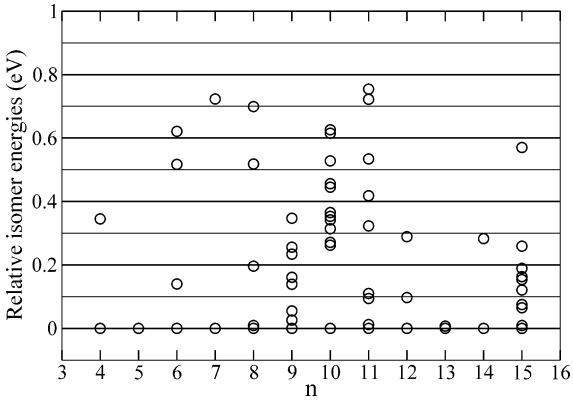

Figure 4. Relative energies of isomers of Al_n.

Table 2. Lowest Vibrational Frequency (cm^{-1}) of Al_n, Al_n^+, and Al_n^- in their Lowest Energy Structure and Spin State

n	0	+	−	n	0	+	−
4	74	42	104	10	55	45	59
5	45	30	16	11	24	38	41
6	32	31	38	12	32	45	32
7	50	52	38	13	26	0	36
8	38	31	57	14	17	25	21
9	28	28	14	15	38	28	50

structures were considered. Their predicted GM for the neutrals $n = 4-10$ agree remarkably well with our GM, except $n = 6$ where they predict a distorted octahedron. There also appears to be small differences in bond lengths for $n = 7$ and 8. Agreement between their GM structures and ours is not very good for anions and cations, but Al_9^- and Al_{10}^- look almost identical. Although they differ in details, there is a resemblance between the B3LYP GM of Sun et al. and our BPW91 GM for Al_n^+ and Al_n^-: in general, structures are not very compact, they have low symmetry, and in many cases there are Al atoms with a low coordination.

The evolution of average nearest-neighbor distance (R_{nn}) (Figure 2) and mean coordination (Figure 3) with cluster size in Al_n are like those given by Rao and Jena[12] but with small differences. The cations have shorter R_{nn} than the neutrals for $n = 4$, 8−11, and this is accompanied by smaller mean coordination (except for $n = 10$). As expected, the curves for neutral and charged clusters in Figures 2 and 3 get close at larger n. The mean coordination of atoms is smaller in Al_n clusters than in Li_n at all sizes.[5] It is smaller than in Be_n up to $n = 10$ roughly, then it becomes comparable to Be_n.[6] As n increases, the hybridization in Al clusters gradually evolves from s^2p^1 to s^1p^2, and the metal character of Al_n develops.[12] As a result, with increasing n, Al_n clusters gradually adopt more compact structures and mean coordinations that are close to maximal and typical of clusters of simpler metals like Li_n and Ag_n.

In our studies of Li[5] and Be[6] clusters, we noted a correlation between the shape (oblate, prolate, quasi-spherical) of the GM found by first-principles and the predicted optimal shape in the ellipsoidal jellium model (EJM). No such correlation is found here for Al_n clusters, no matter whether we take the number of itinerant electron per atom to be 1 or 3. For example, the shape parameter $\eta = (2I_b - I_a - I_c)/I_a$, where $I_a \geq I_b \geq I_c$ are the three moments of inertia of a cluster, equals −0.11 for Al_9 which shows that it is oblate, but the EJM predicts a prolate optimal structure for both 9 and 27 electrons.

Second energy derivatives and vibrational frequencies (Table 2) confirm that all structures in Figure 1 are minima, except maybe Al_{13}^+ for which the lowest frequency is essentially zero and surely lower than the numerical accuracy of the calculations. The highest frequencies for each cluster (not shown in Table 2) cover a range from 260 cm^{-1} in Al_4 to 370 cm^{-1} in Al_5. With the exception of $n = 5$, the highest frequency goes up from a 273 cm^{-1} average for the three $n = 4$ species, to 291 cm^{-1} ($n = 6$), and to 304 cm^{-1} ($n = 7$). The $n = 5$ species have unusually high vibrational frequencies which must be a result of their quasi-planarity and presence of triangles in the structure: the highest frequency of each species is 370 cm^{-1} (Al_5), 359 cm^{-1} (Al_5^+), and 351 cm^{-1} (Al_5^-). There is a jump from 304 cm^{-1} ($n = 7$) to 338 cm^{-1} at $n = 8$, and thereafter the highest frequencies remain roughly constant and inside the range 322−366 cm^{-1} for the 24 species with $n > 7$. This is a manifestation of the fact that the change in hybridization (and bonding nature of orbitals) is almost complete by $n = 8$.[12] Note that the first interior atoms show up at larger size, roughly $n = 12$, and that has no clear effect on vibrational frequencies. Table 3 shows the frequencies of modes for which the calculated IR intensity is larger than 10 km/mol. Those are often, but not always, the highest frequency modes. We also list all frequencies for the more stable cluster ions Al_7^+ and Al_{13}^- at the bottom of Table 3.

Table 3. Most Intense IR Active Vibrational Modes and All Vibrational Frequencies of Al_7^+ and Al_{13}^- with Most IR Intense Shown in Boldface

cluster	frequencies (cm^{-1})
Al_n	$n = 11$: 296; $n = 12$: 331; $n = 13$: 319, 343; $n = 14$: 150, 342
Al_n^+	$n = 4$: 264; $n = 5$: 359; $n = 8$: 144, 322; $n = 9$: 211, 312; $n = 10$: 331, 336; $n = 11$: 278, 279, 296, 298, 315; $n = 12$: 313; $n = 13$: 311, 315; $n = 14$: 313, 324, 338; $n = 15$: 332, 347
Al_n^-	$n = 13$: 168, 169, 176
Al_7^+	52, 58, 107, 176, 177, 181, **232**, 240, 241, **249**, **250**, **259**, 290, 291, 291
Al_{13}^-	35, 60, 61, 68, 68, 115, 115, 128, 129, 129, **168**, **169**, **176**, 189, 192 202, 202, 204, 205, 209, 209, 215, 240, 250, 250, 267, 267, 269, 269, 292, 315, 317, **336**

So far we discussed only the lowest energy minima (GM), but typical TSDS runs end with 10−20 local optimizations that produce anywhere between 1 and 20 distinct minima. In TSDS, diversity in geometric structures is explicitly encouraged. This not only prevents the algorithm from converging too quickly to a single low-energy structure that may not be the GM but also increases the chances of discovering the second, third, ..., most stable isomers. This is a good feature of TSDS because, when comparing to experiments, it is important to look at energy minima that are slightly above the lowest one and get a sense for possible cluster isomers. The energies of Al_n isomers found by TSDS that are within 1.0 eV of the GM but differ from each other by at least 0.01 eV are displayed in Figure 4. Considering that our calculated relative energies are probably not more accurate than 0.2 eV, and room temperature is roughly 0.025 eV, the presence of different cluster isomers is very likely for most cluster sizes except $n = 4$, 5, 7, 10, 13, 14. We will not discuss the structures and properties of isomers other than the GM here as it would be tedious. But those isomers would have to be examined carefully if one had to assign a spectrum for structural determination of specific cluster species.

Local optimization of the neutral Al_n clusters with the SVWN5 exchange-correlation functional yielded the same global minima as with the BPW91 functional except for a few things. The GM of Al_6 in SVWN5 is a edge-capped square pyramid with C_s symmetry. The GM of Al_{12} in

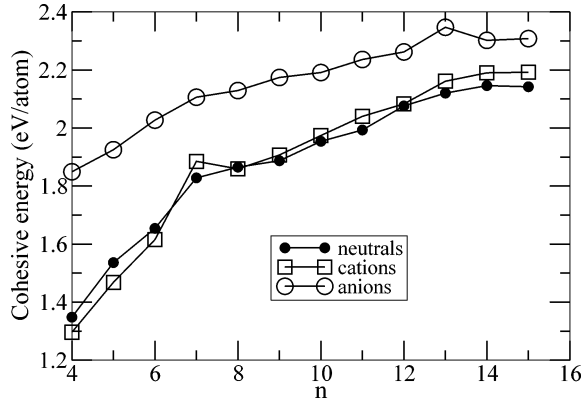

Figure 5. Cohesive energies of neutral and charged aluminum clusters.

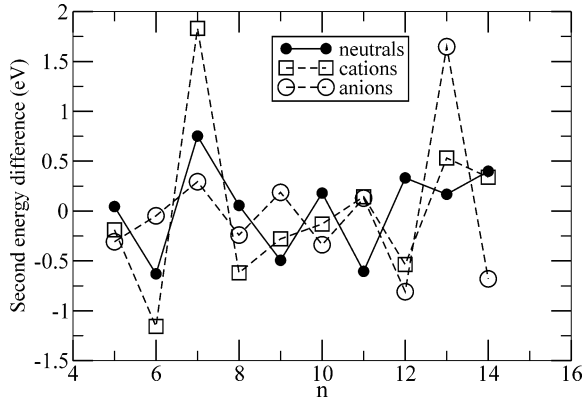

Figure 6. Second energy difference, $\Delta E(n) = E(n+1) + E(n-1) - 2E(n)$, of neutral and charged aluminum clusters.

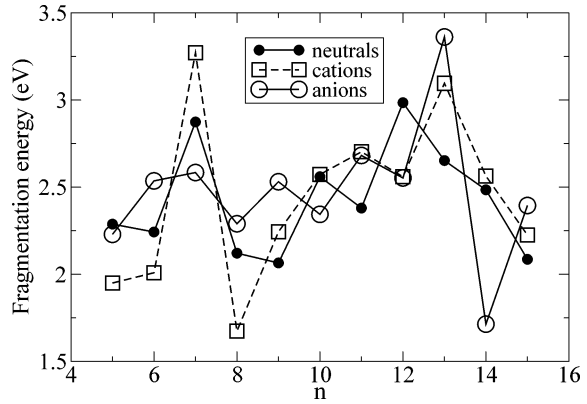

Figure 7. Fragmentation energy of neutral and charged aluminum clusters for the lowest energy fragmentation channel (see text).

SVWN5 is different from BPW91 but is similar to it: it has a central atom with a coordination of 11 and some atoms with low coordination (two atoms with coordination of 4). The GM of Al_7, Al_{13}, and Al_{15} obtained by SVWN5 are topologically equivalent to the BPW91 GM of Figure 1 but with fairly large distortions. The GM we find for the other neutral clusters are virtually identical in SVWN5 and BPW91, but one should bear in mind that GM are obtained by local optimization, with either SVWN5 or BPW91, of the same set of initial structures generated by TSDS/SVWN5 global optimization. A search done entirely with BPW91 (TSDS with BPW91 followed by local optimization with BPW91) might yield different BPW91 structures having lower energy. Still, similarities between the two sets of neutral cluster GM structures found here, and similarities to the GM found in previous KS-DFT studies, indicate that the structures and relative isomer energies do not depend strongly on the choice exchange-correlation functional.

B. Binding Energies. Trends in energies as a function of cluster size are shown in Figures 5−7. The quantities plotted are energies of the following reactions. The cohesive energy is for

$$(1/n)\mathrm{Al}_n \rightarrow \mathrm{Al}$$

$$(1/n)\mathrm{Al}_n^+ \rightarrow ((n-1)/n)\mathrm{Al} + (1/n)\mathrm{Al}^+$$

$$(1/n)\mathrm{Al}_n^- \rightarrow ((n-1)/n)\mathrm{Al} + (1/n)\mathrm{Al}^-$$

the second energy difference corresponds to

$$2\mathrm{Al}_n \rightarrow \mathrm{Al}_{n+1} + \mathrm{Al}_{n-1}$$

$$2\mathrm{Al}_n^+ \rightarrow \mathrm{Al}_{n+1}^+ + \mathrm{Al}_{n-1}^+$$

$$2\mathrm{Al}_n^- \rightarrow \mathrm{Al}_{n+1}^- + \mathrm{Al}_{n-1}^-$$

and the fragmentation energy along the energetically most favored dissociation channel corresponds to

$$\mathrm{Al}_n \rightarrow \mathrm{Al}_{n-1} + \mathrm{Al}$$

$$\mathrm{Al}_n^+ \rightarrow \mathrm{Al}_{n-1}^+ + \mathrm{Al} \text{ or}$$

$$\rightarrow \mathrm{Al}_{n-1} + \mathrm{Al}^+$$

$$\mathrm{Al}_n^- \rightarrow \mathrm{Al}_{n-1}^- + \mathrm{Al}$$

The cohesive energies of neutrals and cations are always close, with cations having a lower cohesive energy at $n < 7$ and higher cohesive energy at $n \geq 7$. The difference is pronounced for Al_7 and Al_7^+ because the latter has a closed electronic shell (20 electrons) in the jellium model. Dissociating Al_n^+ into $(n-1)$ Al atoms and Al^+ concentrates the positive charge onto a single atomic cation which is energetically more costly as n gets larger, and this is why the cations curve eventually crosses above the neutrals curve. Cohesive energies of anion clusters are higher still because the atomic anion Al^- is relatively unstable. Otherwise, these curves are typical of cluster cohesive energies except for conspicuous peaks at Al_7^+ and Al_{13}^-. The second energy differences, and fragmentation energies, also indicate that Al_7^+ (20 electrons) and Al_{13}^- (40 electrons) are particularly stable. This has been noted before,[12] of course, and is well understood in terms of the closed electronic shells of the jellium. Interestingly, all three species (neutral, cation, anion) are relatively stable at $n = 7$ and $n = 13$ by the criterion set by Figure 6. If these energies were known but the structures were not, it would be tempting to explain the stability at $n = 7$ and 13 by closing of atomic shells[21] with a pentagonal

bipyramid (PBP, $n = 7$) and icosahedron ($n = 13$). But as Figure 1 shows, none of the $n = 7$ species is a PBP, and none of the 13-atom species is an icosahedron (Al_{13} and Al_{13}^- are decahedra). A better explanation may be that stability is associated not only with closed electronic shells ($N_e = 20, 40$) but also, to a lesser extent, with numbers of electrons just above and below the shell closing numbers. If this view is correct, simultaneous stability of the neutral, anion, and cation of a given size can happen only for clusters of elements having more than one itinerant electron per atom. It should occur for $N_e = 20, 40, 58$[7] or the combinations M_n (M = valence of the element, n = number of atoms in the cluster): 2_{10}, 2_{20}, 2_{26}, 3_7, 3_{13}, 3_{19}, 4_5, and 4_{10}.

There is a even−odd oscillation in the energy differences of Figure 6, but it is not perfect and it is not as pronounced as for s-valent metals like Li or Ag. Species with even number of electrons are more stable only for $n \geq 8$ in the neutrals series, $n \geq 6$ for anions, and $n = 10$ breaks the expected pattern in the cations series. The favored fragmentation channel according to our calculations is always $(n-1) + 1$ for neutrals and $(n-1)^- + 1$ for anions. For cations we find the lowest dissociation energy pathway for $n = 5-9$ yields Al^+ and Al_{n-1} except at $n = 8$ and find that the products are Al and Al_{n-1}^+ for $n = 8$ and $n > 9$. Note that the exception ($n = 8$) produces the stable cluster ion Al_7^+. This is in line with a suggestion by Martínez and Vela[19] that the favored fragmentation route is generally the one giving the hardest fragments, i.e., the fragments with the largest HOMO−LUMO gap. However, hardness is not the only thing that matters. Spreading the positive charge over larger clusters decreases the Coulombic energy, and that is why the preferred dissociation products are Al and Al_{n-1}^+ at $n = 9-15$ and most likely also for $n > 15$. These favored fragmentation channels agree with those of Rao and Jena[12] except Al_9^+ for which they find the lowest dissociation energy leads to Al_8^+ (see the "relaxed" column in their Table 3).

C. Electronic Structure and Electronic Properties. The trends seen in experimental vertical ionization energies (VIEs)[7] are well reproduced in our calculations (Table 1). The range of VIEs is 6.55−5.75 eV in experiment and 6.73−5.87 eV in our calculations. On average, calculated VIEs are higher by roughly 0.15 eV. Experimental VIEs are nearly constant and equal to 6.45 eV inside the group ($n = 4, 5, 6, 8, 9, 13$), they are all close to 6.20 eV for ($n = 7, 10, 11, 12$), and the two VIEs for $n = 14, 15$ are close to 5.75 eV. Calculated VIEs follow this trend, but they are comparatively too low for Al_7 and Al_{13} (by 0.2 eV) and too high for Al_{14} (by 0.25 eV).

Our calculated adiabatic electron detachment energies (ADEs) are compared to those of previous theoretical work and to two experiments in Table 4. Our GM geometries (and energies) differ from those of Rao and Jena[12] for the neutral or the anion in all cases except $n = 4$ and $n = 14$. Yet, our ADEs do not agree with experiment better or worse than the ADEs of Rao and Jena. Note that the discrepancies between the two sets of experimental results are bigger than 0.3 eV in most cases, but discrepancies between the two sets of calculations are smaller than 0.3 eV in most cases.

Table 4. Adiabatic Electron Detachment Energy from Al_n^- (eV)

n	PW	theory[12]	expt 1[11]	expt 2[8]
4	2.13	2.13	1.74	2.20 ± 0.05
5	2.07	2.06	1.82	2.25 ± 0.05
6	2.36	2.56	2.09	2.63 ± 0.06
7	2.07	2.04	1.96	2.43 ± 0.06
8	2.24	2.56	2.22	2.35 ± 0.08
9	2.71	2.54	2.47	2.85 ± 0.08
10	2.49	2.64	2.47	2.70 ± 0.07
11	2.79	2.64	2.53	2.87 ± 0.06
12	2.36	2.31	2.53	2.75 ± 0.07
13	3.07	3.38	2.86	3.62 ± 0.06
14	2.30	2.30	2.47	2.60 ± 0.08
15	2.61	2.70	2.53	2.90 ± 0.08

The HOMO−LUMO gaps (eV) for the neutral clusters are, in order of increasing size, as follows: 0.30 ($n = 4$), 0.85, 0.74, 0.81, 0.97 ($n = 8$), 0.67, 0.82, 0.63, 1.04 ($n = 12$), 0.74, 0.94, and 0.63 ($n = 15$). The variations are not strong, but the highest gap ($n = 12$) does correspond to a relatively stable cluster. The two magic clusters have the largest gap as expected, 1.57 eV (Al_7^+) and 1.45 eV (Al_{13}^-).

Like Rao and Jena, we find that most Al clusters with $n > 3$ have ground states with the lowest possible multiplicity. However, Rao and Jena found many more exceptions to that trend, that is, clusters that have the next lowest possible multiplicity in their ground state. They are Al_4, Al_4^+, Al_5^+, Al_6, Al_8, and Al_{10}. By contrast, the only high-spin clusters that we found are Al_4, Al_4^+, and Al_7^-. We must add, however, that the energy difference between high-spin and low-spin energy minima are sometimes very small. They are, in eV, as follows: Al_4 (−0.29), Al_4^+ (−0.08), Al_5^+ (0.00), Al_6 (+0.01), Al_7^- (−0.08), and Al_8 (+0.31). Stern-Gerlach experiments by Cox et al.[22] showed that spin multiplicities of neutral Al clusters are 2 for odd n and 3 for even n up to $n < 9$. Here, improving the theoretical geometric structures (of Al_6 and Al_8) seemingly worsens agreement with experiment. It may be that the BPW91 level of theory and TSDS geometry optimization are still not up to the task of predicting magnetism in small Al clusters or that low-lying isomers complicate the interpretation of magnetic properties so that magnetic moments are of little use for structure assignments.

IV. Conclusion

Global optimization of Al cluster geometries was done with the same energy method (BPW91/LANL2DZ) as in a previous work. Detailed comparison of our results with that previous work gives two main conclusions. First, without guiding principles it is very difficult to find the GM of clusters, even for small clusters ($n \leq 8$). Finding the GM (or good approximations) requires an efficient and unbiased search algorithm coupled with an accurate energy function. Here we found 24 structures that improve upon previously published structures. We want to point out that the way in which the GM were searched in the earlier work[12] is not at all unusual: many theoretical studies have used this approach. Second, it is very difficult to learn about the

geometric structure of metal clusters by comparing experimental and theoretical data about their electronic properties (magnetic moments, ionization energies, electron detachment energies). That is because the jellium model works rather well: electronic properties are largely controlled by the number of electrons, not by the positions of the nuclei. Here, the GM we found for Al_n, Al_n^+, and Al_n^- differ significantly from previous work,[12] but our calculated properties (preferred fragmentation channels, ionization energies, electron detachment energies, magnetic moments) do not differ much. Theoretically our results are better, but they do not agree with experiment better, and uncertainties (experimental and computational) blur any conclusion we could make about specific structure assignments.

Comparison of structures to other first-principles studies that used different basis sets and functionals[16,17] show many similarities in the predicted GM structures but differences in details. On the other hand, GM structures predicted using empirical potentials[14,15] are completely at odds with our results. They are more compact and more symmetrical than first-principles structures and that is probably due to the inability of those empirical potentials to model the change in sp hybridization as a function of atom coordination. For aluminum clusters, the GM of empirical potentials differ too much from those of KS-DFT to be useful as an initial guess for searching KS-DFT energy surfaces.

It will be very difficult to elucidate with confidence the structure of larger ($n > 7$) Al clusters by comparison of the calculated properties of different theoretical isomers to measured properties, for three reasons. First, as we already said, our calculated properties agree no better with experiment than those of Rao and Jena[12] although our GM structures are very different and theoretically better. Second, as Figure 4 shows, there are often many cluster isomers for a given size, and finding all those isomers and computing reliably their properties is a challenge. Third, calculating relative isomer energies with quantitative accuracy[23] (0.01 eV/atom or better) requires computational methods that are impractical and much more costly than what we used here. Structure elucidation for all but the smallest Al clusters will probably require rich and accurate experimental data that are sensitive to geometry (vibrational or well resolved photoelectron spectra for instance), in combination with a computational study that includes an extensive search for the GM and low-lying energy isomers by a first-principles method and a calculation of relative energies and cluster properties with the best possible level of theory.[24]

Finally, our results confirm that Al_7^+ and Al_{13}^- have special stability and larger HOMO−LUMO gaps as a result of their electron count (20 and 40) matching a shell closing in the jellium model. However, the jellium model does not help understand the evolution of geometries with size.

Acknowledgment. This work was supported by the Natural Sciences and Engineering Research Council of Canada.

References

(1) Chekmarev, S. F. *Phys. Rev. E* **2001**, *64*, 036703−036703-9. Tsai, C. J.; Jordan, K. D. *J. Phys. Chem.* **1993**, *97*, 11227−11237.

(2) Roberts, C.; Johnston, R. L.; Wilson, N. T. *Theor. Chem. Acc.* **2000**, *104*, 123−130.

(3) Gendreau, M. In *Handbook of Metaheuristics*; Glover, F., Kochenberger, G. A., Eds.; Kluwer: Dordrecht, The Netherlands, 2003; pp 37−54.

(4) Chen, J.; Fournier, R. *Theor. Chem. Acc.* **2004**, *112*, 7−15.

(5) Fournier, R.; Cheng, J.; Wong, A. *J. Chem. Phys.* **2003**, *119*, 9444−9454.

(6) Sun, Y.; Fournier, R. *Comput. Lett.* **2005**, *1*, 210−219.

(7) Schriver, K. E.; Persson, J. I.; Honea, E. C.; Whetten, R. L. *Phys. Rev. Lett.* **1990**, *64*, 2539−2542.

(8) Li, X.; Wu, H.; Wang, X.-B.; Wang, L.-S. *Phys. Rev. Lett.* **1998**, *81*, 1909−1912.

(9) Jarrold, M. F.; Bower, E. J.; Kraus, J. S. *J. Chem. Phys.* **1987**, *86*, 3876−3885. Hanley, L.; Ruatta, S. A.; Anderson, S. L. *J. Chem. Phys.* **1987**, *87*, 260−268. Saunders, W. A.; Fayet, P.; Wöste, L. *Phys. Rev. A* **1989**, *39*, 4400−4405.

(10) Leuchtner, R. E.; Harms, A. C.; Castleman, A. W., Jr. *J. Chem. Phys.* **1991**, *94*, 1093−1101.

(11) Taylor, K. J.; Pettiette, C. L.; Graycraft, M. J.; Chesnovsky, O.; Smalley, R. E. *Chem. Phys. Lett.* **1988**, *152*, 347−352.

(12) Rao, B. K.; Jena, P. J. *Chem. Phys.* **1999**, *111*, 1890−1904.

(13) Salahub, D. R.; Messmer, R. P. *Phys. Rev. B* **1977**, *16*, 2526−2536.

(14) Sebetci, A.; Güvenç, Z. B. *Modell. Simul. Mater. Sci. Eng.* **2005**, *13*, 683−698.

(15) Lloyd, L. D.; Johnston, R. L. *Chem. Phys.* **1998**, *236*, 107−121.

(16) Jones, R. O. *J. Chem. Phys.* **1993**, *99*, 1194−1206.

(17) Sun, J.; Lu, W. C.; Wang, H.; Li, Z.-S.; Sun, C.-C. *J. Phys. Chem. A* **2006**, *110*, 2729−2738.

(18) Akola, J.; Häkkinen, H.; Manninen, M. *Phys. Rev. B* **1998**, *58*, 3601−3604.

(19) Martínez, A.; Vela, A. *Phys. Rev. B* **1994**, *49*, 17464−17467.

(20) Frisch, M. J.; Trucks, G. W.; Schlegel, H. B.; Scuseria, G. E.; Robb, M. A.; Cheeseman, J. R.; Montgomery, J. A., Jr.; Vreven, T.; Kudin, K. N.; Burant, J. C.; Millam, J. M.; Iyengar, S. S.; Tomasi, J.; Barone, V.; Mennucci, B.; Cossi, M.; Scalmani, G.; Rega, N.; Petersson, G. A.; Nakatsuji, H.; Hada, M.; Ehara, M.; Toyota, K.; Fukuda, R.; Hasegawa, J.; Ishida, M.; Nakajima, T.; Honda, Y.; Kitao, O.; Nakai, H.; Klene, M.; Li, X.; Knox, J. E.; Hratchian, H. P.; Cross, J. B.; Bakken, V.; Adamo, C.; Jaramillo, J.; Gomperts, R.; Stratmann, R. E.; Yazyev, O.; Austin, A. J.; Cammi, R.; Pomelli, C.; Ochterski, J. W.; Ayala, P. Y.; Morokuma, K.; Voth, G. A.; Salvador, P.; Dannenberg, J. J.; Zakrzewski, V. G.; Dapprich, S.; Daniels, A. D.; Strain, M. C.; Farkas, O.; Malick, D. K.; Rabuck, A. D.; Raghavachari, K.; Foresman, J. B.; Ortiz, J. V.; Cui, Q.; Baboul, A. G.; Clifford, S.; Cioslowski, J.; Stefanov, B. B.; Liu, G.; Liashenko, A.; Piskorz, P.; Komaromi, I.; Martin, R. L.; Fox, D. J.; Keith, T.; Al-Laham, M. A.; Peng, C. Y.; Nanayakkara, A.; Challacombe, M.; Gill, P. M. W.; Johnson, B.; Chen, W.; Wong, M. W.; Gonzalez, C.; Pople, J. A. *Gaussian 03, Revision C.02;* Gaussian, Inc.: Wallingford, CT, 2004.

(21) Martin, T. P. *Phys. Rep.* **1996**, *273*, 199−241.

(22) Cox, D. M.; Trevor, D. J.; Whetten, R. L.; Rohlfing, E. A.; Kaldor, A. *J. Chem. Phys.* **1986**, *84*, 4651−4656.

(23) Schultz, N. E.; Staszewska, G.; Staszewski, P.; Truhlar, D. G. *J. Phys. Chem. B* **2004**, *108*, 4850−4861.

(24) Martínez, A.; Sansores, L. E.; Salcedo, R.; Tenorio, F. J.; Ortiz, J. V. *J. Phys. Chem.* **2002** *106*, 10630−10635. Wu, H.; Li, X.; Wang, X.; Ding, C. F.; Wang, L. S. *J. Chem. Phys.* **1998**, *109*, 449−458.

CT6003752